J Ther Eng, Vol. 12, No. 2, pp. 466−483, March, 2026

Journal of Thermal Engineering
Web page info: https://jten.yildiz.edu.tr
DOI: 10.14744/thermal.0001092

Research Article

Performance analysis of solar still with separate evaporatively cooled condenser

Niladri SARKAR[1], Aneesh SOMWANSHI[2], Anil Kr. TIWARI[1,*]

[1]*Department of Mechanical Engineering, National Institute of Technology, Raipur, 490042, India*
[2]*Department of Mechanical Engineering, MATS University Raipur, 490042, India*

ARTICLE INFO

Article history
Received: 13 May 2025
Revised: 07 October 2025
Accepted: 26 October 2025

Keywords:
Air Cooler; Distillate Output; Economic Analysis; Separate Condenser; Solar Still

ABSTRACT

Potable water scarcity is a serious global issue, and solar stills provide an eco-friendly way to produce clean water using sunlight. Their efficiency mainly depends on the temperature difference between the basin water and the glass cover. Adding an external condenser helps to boost this difference by keeping the condensation surface cooler, leading to more water output. Actively cooling the condenser can enhance this effect even further, significantly improving the distillate yield. In this study, the performance of a single-slope solar still with a separate condenser integrated into an air cooler system was investigated. A low-power exhaust fan directs the moist air towards the condenser. The condenser plate is cooled by water from the air cooler's tank, which flows over it. This evaporatively cooled condenser enhances the condensation process, leading to increased overall productivity of the solar still. Mathematical model of the design was created and validated through experiments. Effect of parameters like water depth, mass flow rate of water over condenser, relative humidity and wind velocity of air on stills performance has been investigated. The depth of water in the solar still's basin has very little impact on the distillate produced. When the depth of water in basin increased from 1cm to 5cm the total daily distillate output is decreased only by 4.9%. The mass flow rate of water flowing over condenser has very negligible effect on still's performance. Unlike conventional still with increase in wind velocity from 1m/s to 4m/s the hourly distillate output decreases by 2.7%. With increase in humidity of air the output decreases. In Raipur, Chhattisgarh (India) for months of May (summer), January (winter), and October (autumn) the system produced 7.83 kg, 3.45 kg and 5.30 kg of distilled water daily. The water is produced at a reasonable cost of Rs. 1.30/kg (US$ 0.0151/kg). Due to continuous cooling of condenser, the system is able to generate some amount of water even in night time.

Cite this article as: Sarkar N, Somwanshi A, Tiwari AK. Performance analysis of solar still with separate evaporatively cooled condenser. J Ther Eng 2026;12(2):466−483.

***Corresponding author.**
*E-mail address: aktiwari.mech@nitrr.ac.in

This paper was recommended for publication in revised form by Editorin-Chief Ahmet Selim Dalkılıç

INTRODUCTION

Freshwater scarcity is an escalating challenge as population growth, urbanization, and industrial activity strain conventional sources. In many regions, declining rainfall, over-drawn aquifers, and rising salinity now limit supplies for both drinking and agriculture. Salinity in particular reduces soil fertility and crop yields, while pollutants from industry, sewage, and agricultural runoff further degrade surface and groundwater quality. These factors collectively heighten public-health risks and sustain the burden of water-borne disease. Numerous high and medium-tech techniques for purifying water that rely on conventional energy sources have been developed as a result of scientific and technological advancements. But "solar distillation" stands out as an easy, economical, and ecologically acceptable method for generating drinkable water that is dependent on renewable energy sources rather than traditional energy sources. A device that uses solar energy to clean water is called solar still (SS). Its principle is basically vaporization and condensation. Several designs for passive solar stills have been extensively investigated and examined by researchers in an effort to increase their efficiency. The designs include inverted absorber solar still, floating solar still, and hybrid membrane solar stills powered by fossil fuel [1-8].

Recent studies have shown growing interest in improving the efficiency of solar stills, particularly through design modifications like adding external condensers, using nanomaterials, using PCM, or coupling with other renewable systems. These advancements aim to boost water output and address limitations like low productivity [9-17]

In a SS, solar energy heats impure or salty water, causing it to evaporate. The water vapour then condenses on a cool surface and is collected as pure water, leaving behind impurities and salts. The temperature difference between the water (T_w) in basin and condenser surface (T_c) is the driving factor responsible for getting pure water (condensate). Studies [18–22] have demonstrated that the difference in temperature between the water (where evaporation takes place) and condenser (T_w-T_c) is decreased when water vapour condenses inside a solar still.

It has been suggested that the condenser and the SS chamber be separated in order to increase this temperature differential. In this configuration, water vapour passes from the main chamber of the solar still into a condensation chamber that is separated from the main chamber (SS chamber). As a result, the still's glass surface experiences relatively little condensation. The (T_w-T_c) between the evaporative and condenser rises as a result of the majority of condensation occurring in the condensing chamber, which accelerates evaporation and increases distillate output [23–32]. This design of SS was called as SS with separate condenser (SSSC).

The impact of integrating a connected passive condenser on a passive solar still's efficiency was investigated by Fath and Elsherbiny [23]. They used both theoretical analysis and experimental in their approach to this subject. Diffusion, purging, and spontaneous circulation are the three mass transfer modes in a solar still-condenser system that the researchers examined. The diffusion and purging modes were the focus of their studies, and they discovered that the outcomes closely matched the theoretical expectations. They claimed that employing the separate condenser increased production by almost 70% in purging mode. A SS with an integrated passive condenser and a natural circulation method for humidification and dehumidification was studied by Fath and colleagues [33]. The system produced 5.1L/m^2 each day, according to their research.

Madhlopa and Johnstone's [34] analytical studied on the performance of a passive SS with a separate condenser. They proposed the design consists of three basins: Basin 1 is located in the evaporation chamber and is covered with a glass cover, while Basins 2 and 3 are situated in the condenser chamber. Basin 3 is covered with an opaque condensing cover. Basin 1 produces the first effect, Basin 2 the second effect, and Basin 3 the third effect. When compared to a conventional SS, they found a 62% increase in productivity. Three major components contribute to the total distillate output: the first effect, which has one evaporator basin, makes up 60% of the output; the second effect, which has an additional condenser basin, makes up 22%; and the third effect, which has two additional evaporator basins, makes up 18%.

Monowe et al. [35] proposed, a new design for a portable thermal-electrical solar still with an external condenser and reflecting booster. The system is engineered to reduce the loss of latent heat from condensation by capturing and storing it in the condenser. This stored heat can subsequently be used to operate the still at night or to preheat saline water for household usage. According to preliminary results, the still can operate as efficiently as 77% when the preheated water is used for household use and as efficiently as 85% when the stored heat is used for both nocturnal operation and system recharging with fresh preheated saline water.

A modified SS with an external condenser and an Al_2O_3-water nanofluid was studied by Kabeel et al. [36]. They discovered that when the external condenser was the only one used, the productivity of the solar still improved by 53.2%. When the nanofluid was incorporated along with the external condenser, the productivity enhancement rose to approximately 116%. Rabhi et al. [37] examined the effectiveness of a modified single-basin, (SSSS) with a condenser and pin fins for heat absorption. Their findings showed that using absorber fins on the basin liner was not as effective as incorporating an external condenser. Interestingly, they discovered that, in comparison to a traditional SS, the external condenser increased water productivity by 32.18%. On the other hand, the SS with basic pin fins only had a 14.53% rise.

The thermal performance of an inflatable plastic SS with a passive condenser was investigated by Bhardwaj et al. [38]. According to their findings, the device produced about

0.75 litres of drinkable water every hour. Furthermore, they observed that the water output was increased to more than 0.95 litres per hour by employing airflow over the passive condenser.

Rahmani and Boutriaa [39], performed transient simulation of a basin-type solar still with an external condenser is proposed. The performance of the still is analyzed under the combined influence of wind conditions and varying condenser areas during both winter and summer seasons. The study includes an optimization of the condenser design aimed at maximizing distillate yield. Results indicate that the non-conventional solar still (NCL) achieves a maximum daily yield of 2.71 kg/m² in winter and 4.73 kg/m² in summer. Later, Kabeel et al. [40] provided a thorough analysis of various solar stills that were connected to separate condensers. They come to the conclusion that increasing the area available for condensation raises the rate at which condensation occurs, which in turn raises the rate at which evaporation occurs in the basin. Ultimately, the (T_w-T_c) between the evaporating and condensing zones determines how efficient is the condensation process.

Saini et al. [41] investigated the performance of SSSS integrated with SPV module and passive condenser. The impact of different packing factors β_c=0, 0.25, 0.45, 0.65 and 0.85 β_c=0, 0.25, 0.45, 0.65 on the performance of solar cells using various PV technologies has been studied. For the c-Si SPV module, the maximum overall energy efficiency was found to be 57.5%, 55.2%, 53.4%, 53.1%, and 41.4% for packing factors of 0.85, 0.65, 0.45, 0.25, and 0, respectively. Additionally, the system's productivity was measured and found to be 1.78 kg, 2.83 kg, 3.66 kg, 4.12 kg, and 4.92 kg, 1.78 kg per day for packing factors of 0.85, 0.65, 0.45, 0.25 and 0, respectively

In previous investigations researchers investigated different configurations of SS having separate condenser unit. This unit helps to collect water vapour from SS and condenses it separately beneath condensing plate this helps to enhance overall productivity of SS. With separate condensing unit the rate of water condensation will increase due to lower condenser temperature. Water cooled condenser will further helps to reduce temperature more in comparison to condenser without cooling. This is found to be a notable research gap identified by reviewing different works on solar still having separate condenser. To decrease the temperature of condenser even more here in this work we presented a new design of SS with separate evaporatively cooled condenser. The condenser cover is evaporatively cooled by flowing cool tank water from air coolers tank contributes to decreasing the temperature of condensing cover furthermore and allows more water vapour to condense beneath condensing plate. SS having separate condenser is connected with the tank of an air cooler. The proposed design is an extension of the design proposed by Somwanshi & Tiwari [42]. In their previous design they proposed to connect an air cooler tank by a passive solar still. The cooled tank water from tank of cooler utilized to cool glass cover. Cooling the glass cover of a solar still can greatly increase its efficiency. This raises the temperature differential between the glass cover and the water in the basin, which significantly boosts the still's output. The use of air cooler is very common during summers for space cooling. The water in cooler tank is cooled due to continuous evaporation process. The coolness in tank water remains unutilized. Authors proposed to use this cooled tank water to cool the cover of SS their proposed design helps to get the annual distillate output by 56.5%.

Tiwari and Somwanshi [43] subsequently presented another concept of a small size solar still plant integrated to garden fountain. The concept worked reasonably well to produce reasonable amount of potable water to meet the demand of drinking water in small communities.

In this work we proposed to cool the cover of SS having separate condenser. The condenser unit has been separated and connected with air cooler's tank. The proposed design is shown in Figure 1. The water from condenser cover is collected and recirculated back to air coolers tank.

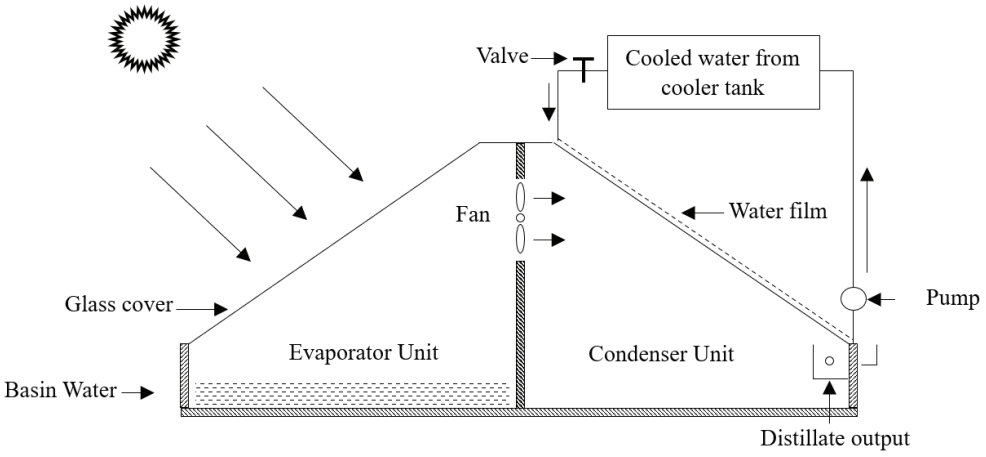

Figure 1. Schematic of the proposed design.

The mathematical model of the proposed system has been created and experimentally validated experiments were carried out at Raipur, Chhattisgarh, India (21.2787° N, 81.8661° E). The effect of parameters like MFR of water flowing over cover, depth of water in the basin, relative humidity of air and wind velocity on the performance of proposed has been investigated. The performance of the proposed system has been investigated for a day in summer (May), winter (Jan) and autumn (October). Economic analysis has been performed to determine the cost of distillate output produced.

MATHEMATICAL ANALYSIS

Thermal network of the proposed system (Fig. 2). and Figure 3 shows different internal and external heat transfer of the proposed still.

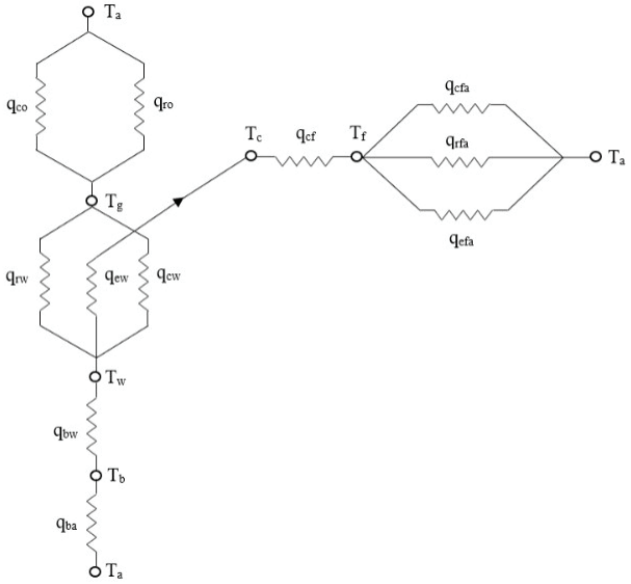

Figure 2. Thermal network of proposed design.

Referring Figure 3 Energy balance equation of proposed system considering unit area are as follows

i. The solar distillation unit is vapour-tight.
ii. The heat capacity of glass, aluminum and condenser is neglected.
iii. The thickness of water film considered very small.

Glass Cover

$$\tau_1 I + q_{rw} + q_{cw} + q_{ew}(1-\phi) = q_{ca} + q_{ra} \quad (1)$$

In Eq.1, ϕ is the fraction of water vapour incident to external condenser, the value of ϕ is considered 1 when all vapours are forced by internal fan towards external condenser.

Eq. 1 can be written as,

$$\tau_1 I + h_{rw}(T_w - T_g) + h_{cw}(T_w - T_g) = h_{ca}(T_g - T_a) + h_{ra}(T_g - T_a) \quad (2)$$

Or,

$$\tau_1 I + h_i(T_w - T_g) = h_o(T_g - T_a) \quad (3)$$

$$h_i = h_{rw} + h_{cw} \quad (4)$$

$$h_o = h_{ca} + h_{ra} \quad (5)$$

Basin Water

$$M_w c_w \frac{dT_w}{dt} = \tau_2 I + q_{bw} - q_{cw} - q_{rw} - q_{ew} \quad (6)$$

Or,

$$M_w c_w \frac{dT_w}{dt} = \tau_2 I + h_b(T_b - T_w) - h_{cw}(T_w - T_g) - h_{rw}(T_w - T_g) - h_{ew}(T_w - T_c) \quad (7)$$

Basin Liner

$$\tau_3 I = q_{bw} + q_{ba} \quad (8)$$

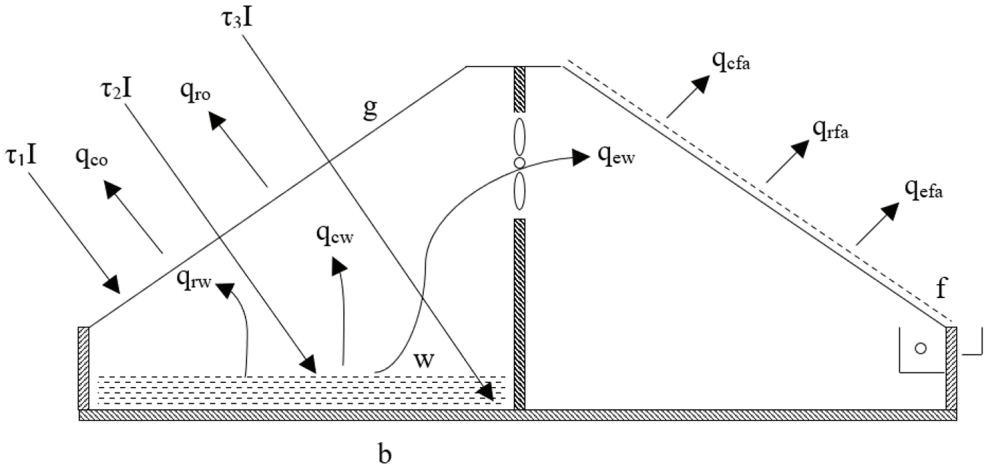

Figure 3. Internal & external heat transfer rate of the proposed still.

Or,

$$\tau_3 I = h_b(T_b - T_w) + U_b(T_b - T_a) \quad (9)$$

Separate Consender

$$q_{ew} = q_{cf} \quad (10)$$

$$h_{ew}(T_w - T_c) = h_f(T_c - T_f) \quad (11)$$

Water Film

Considering the thickness of water film very small the energy balance of strip of thickness (dx) Figure 4, will be

$$\dot{m}_f c_w \frac{dT_f}{dx} dx = \dot{q}_{cf} b dx - \dot{q}_{cfa} b dx - \dot{q}_{rfa} b dx - \dot{q}_{efa} b dx \quad (12)$$

$$m_f c_w \frac{dT_f}{dx} dx = h_f(T_c - T_f) b dx - h_2(T_f - T_a) b dx - 0.013 h_{ca}(P_f - \gamma P_a) \quad (13)$$

From Eq. (3) and Eq. (9) the glass temperature and temperature of basin liner will be given by,

$$T_g = \frac{\tau_1 I + h_i T_w + h_o T_a}{h_i + h_o},\ T_b = \frac{\tau_3 I + h_b T_w + U_b T_a}{h_b + U_b} \quad (14)$$

From Eq. (14) and Eq. (7) we have,

$$\frac{dT_w}{dt} + K_1 T_w = K_2 + K_3 T_c \quad (15)$$

In Eq. 15 the expressions for constants K_1, K_2 and K_3 are given in Appendix-I

Solving Eq. (15) considering the water temperature at time t=0 as T_{c0}

$$T_w = K_4 + K_5 T_c \quad (16)$$

From Eq. (11) and Eq. (16) the value of T_c will be given by,

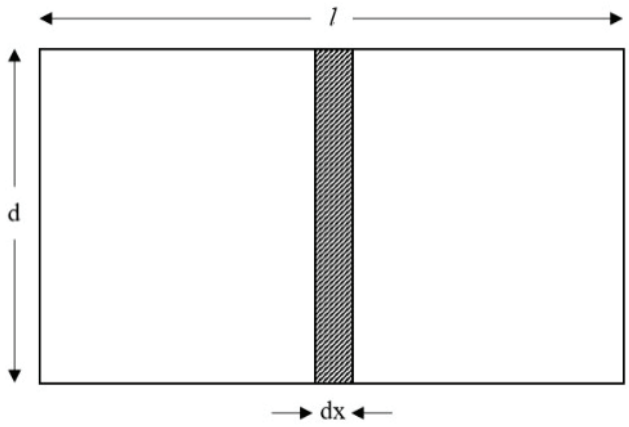

Figure 4. Considering strip of width 'dx'.

$$T_c = K_6 + K_7 T_f \quad (17)$$

Substituting the value of T_c in Eq. 13, we have

$$\frac{dT_f}{dx} = -A T_f^{\,2} + B T_f + C \quad (18)$$

The saturated vapour pressure can be written as,

$$P = R_1 T^2 + R_2 T + R_3$$

The values of R_1, R_2 and R_3 are determined by the fitting (polynomial degree 2) from the saturation vapour pressure table in the temperature range of 7° C to 55° C.

Integrating Eq. 18 we have

$$\frac{T_f - (B/2A) - C_1}{T_f - (B/2A) + C_1} = \beta \exp(-2AC_1 x) \quad (19)$$

In Eq. 19 the value of β and C_1 will be given by,

$$\beta = \frac{T_{f0} - (B/2A) - C_1}{T_{f0} - (B/2A) + C_1}$$

In above equation T_{f0} is the initial film temperature flowing over cover at x=0

The exit film temperature at x=d will be,

$$T_{fe} = (B/2A) + C_1\left[\frac{1 + \beta \exp(-2AC_1 d)}{1 - \beta \exp(-2AC_1 d)}\right] \quad (20)$$

The average film temperature will be given by,

$$T_{fa} = (B/2A) + \frac{1}{Ad} \ln\left[\frac{\exp(2AC_1 d) - \beta}{(1 - \beta)}\right] - C_1$$

By substituting the value of T_{fa} into Equation (17), we can determine the average glass temperature ($\bar{T}_g$), and then obtain the water temperature using Equation (16).

Hourly yield is given by,

$$\dot{m}_{ew} = \frac{h_{ew}(T_w - \bar{T}_c)}{L} \times 3600 \quad (21)$$

The value of various constants and the correlation for determining different heat transfer coefficients used in mathematical model are given in Appendix-II

Expressions for Determine τ_1, τ_2 and τ_3 [18]

$$\tau_1 = (1 - R_g)\alpha_g \quad (22)$$

$$\tau_2 = (1 - R_g)(1 - \alpha_g)(1 - R_w)\alpha_w \quad (23)$$

$$\tau_3 = (1 - R_g)(1 - \alpha_g)(1 - \alpha_w)(1 - R_w)\alpha_b \quad (24)$$

Description of Proposed Design

Figure 1 shows a schematic and a picture of the proposed design. Various dimensions of the design have been

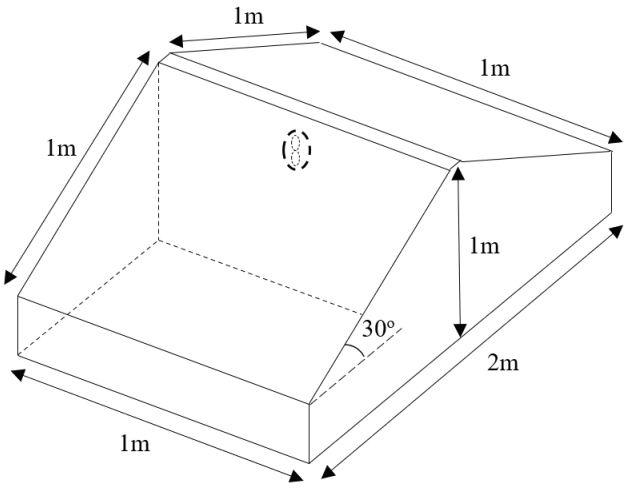

Figure 5. Dimensions of the proposed still.

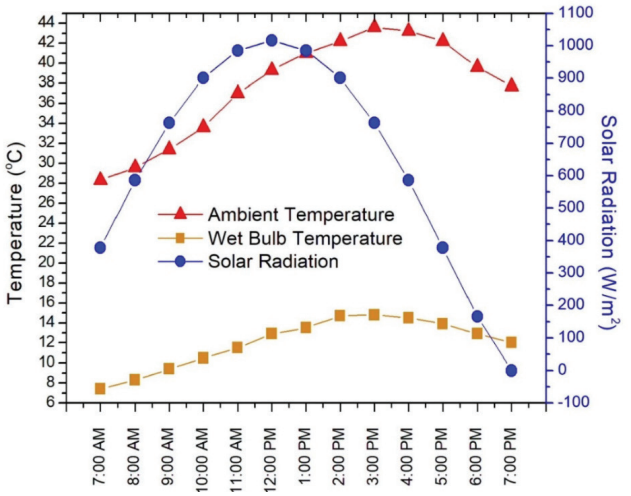

Figure 6. Solar radiation and ambient temperature during the experiment.

shown in Figure 5. The whole setup consists of two different parts separated by an insulated partition. The part at left side is evaporator unit and side towards right is called as condenser unit. A low-power (5W) solar exhaust fan is used to drive the vapours produced by the water in the evaporative chamber absorbing solar energy into the condenser unit. The condenser plate is made of aluminum sheet and it is continuously cooled by cooled tank water pumped from the cooler tank connected with condenser unit. With flow of cooled water (inlet temperature equal to WBT of ambient air) the condenser helps to carry the heat generated by vapours condensed in the bottom of the condenser plate. As a result, the condenser cover and basin water have a greater temperature differential. Both the condenser unit and the glass cover (evaporator unit) have a surface area of one metre square.

The water flowing over condenser is collected and recirculated back to cooler tank. To maintain the mass flow rate of water flowing over condenser a valve has been provided with inlet pipe (Fig.1) The hot water recirculated back to cooler tank is not going to affect the performance of air cooler [44].

Validation of Model

To validate the proposed mathematical model, an experiment was carried out on May 22, 2023, at Raipur, Chhattisgarh, India (21°14′40″N, 81°37′50″E). The hourly solar radiation and ambient temperature and relative humidity during experiment is recorded and shown in Figure 6. An image of the experimental setup is shown in Figure 7, and Table 1 lists the specifics of the instruments used in the experiment. The uncertainty of various

Figure 7. Photograph of the experimental setup.

Table 1. Various instrument used during experiment

Range	Instrument
0°C to 150°C	Temperature sensor K type- constantan
-50°C to 199.9°C	RTD- Platinum temperature sensor
0.0m/s to 45.0m/s	Digital anemometer
0W/m² to 1500W/m²	Pyranometer (Kipps and Zenon)

instruments utilized in experiment is shown in Table 2. The initial temperatures of the water, glass cover, and condensing cover were noted before the experiment started. The mass flow rate (MFR) of the cooled water passing over the condensing cover was measured at 0.065 kg/s, while the water depth in the solar still's (SS) basin was kept at 2 cm.

From 7:00 AM to 7:00 PM, hourly readings of the basin water, glass cover, and condensing cover temperatures were taken. A mathematical model was used to determine the corresponding theoretical values for the temperature of the condensing cover, glass cover, and basin water. The experimental results nearly match the theoretical values, as seen in Figure 8, 9, 10 and 11. Root mean square of percentage deviation e represents the closeness of the theoretical and experimental values. 'e' is given by [13],

$$e = \sqrt{\frac{\sum (e_x)^2}{n}}$$

$$e_x = [\frac{X_{pre(x)} - X_{\exp t(x)}}{X_{pre(x)}}] \times 100$$

The correlation between the predicted values and experimental values is given by coefficient of correlation (r). The correlation coefficient is given by the following equation

$$r = \frac{N\sum X_{pr}X_{\text{ex}} - (\sum X_{pr})(\sum X_{\text{ex}})}{\sqrt{N\sum X_{\text{ex}}{}^2 - (\sum X_{\exp})^2}\sqrt{N\sum X_{pr}{}^2 - (\sum X_{pr})^2}}$$

The experimentally measured water temperatures closely match the computed values. The standard error ("e") ranges from 6.79 to 8.55, while the correlation coefficient ("r") lies between 0.998 and 0.999, indicating an excellent fit between the theoretical and experimental results (see Figs. 8–10). This confirms that the model predicts water temperature with high accuracy. However, the deviation between theoretical and experimental distillate yield is higher, at about 14.6 %. For solar distillation systems, such a difference is generally considered acceptable while calculate the distillate output. Moreover, as shown Table 2, the combined total uncertainty of all measurement instruments is 2.661 %. This low level of uncertainty indicates that the reported trends and the solar still's performance remain reliable, and the small variations do not significantly affect the conclusions drawn from the study.

Table 2. Uncertainty analysis

Uncertainty Parameters	Uncertainty
Temperature (U_T) K thermocouple [Sensor accuracy (sa), calibration (c), Resolution (R), Repeatability (Re)]	$U_T = [U_{sa}^2 + U_c^2 + U_R^2 + U_{\text{Re}}^2]^{1/2}$ $U_T = [1.27^2 + 0.29^2 + 0.058^2 + 0.3^2]^{1/2} = 1.338$
Temperature (U_{T1}) RTD [Sensor accuracy (sa), calibration (c), Resolution (R), Repeatability (Re)]	$U_{T1} = [U_{sa}^2 + U_c^2 + U_R^2 + U_{\text{Re}}^2]^{1/2}$ $U_{T1} = [0.202^2 + 0.115^2 + 0.029^2 + 0.1^2]^{1/2} = 0.255$
Air velocity Measurement U_A [Accuracy(a), Calibration (c), Resolution (R), *Reeability* (Re)	$U_A = [U_a^2 + U_c^2 + U_R^2 + U_{\text{Re}}^2]^{1/2}$ $U_A = [0.087^2 + 0.043^2 + 0.029^2 + 0.1^2]^{1/2} = 0.142$
Mass flow rate (U_m)	$U_m = [(\frac{\Delta V}{V})^2 + (\frac{\Delta t}{t})^2]^{1/2}$ $U_m = [(\frac{0.0001}{0.010})^2 + (\frac{1}{154})^2]^{1/2} = 0.0119$
Solar Radiation (U_s) [Calibration (c), Cosine error (co), Repeatability (Re)]	$U_s = [U_c^2 + U_{co}^2 + U_{\text{Re}}^2]^{1/2}$ $U_s = [1^2 + 2^2 + 0.5^2]^{1/2} = 2.291$
Total Uncertainty U_o	$U_o = [U_T^2 + U_{T1}^2 + U_A^2 + U_m^2 + U_s^2]^{1/2}$ $U_o = [1.338^2 + 0.255^2 + 0.142^2 + 0.019^2 + 2.291^2]^{1/2}$ $U_o = \pm 2.661\%$

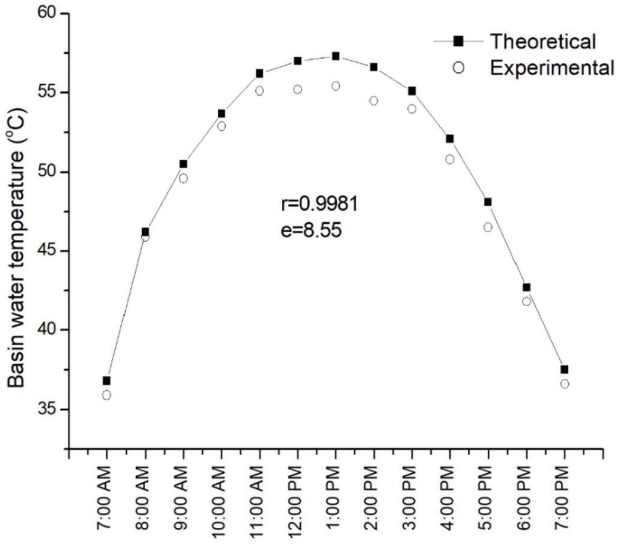

Figure 8. Theoretical and experimental water temperature.

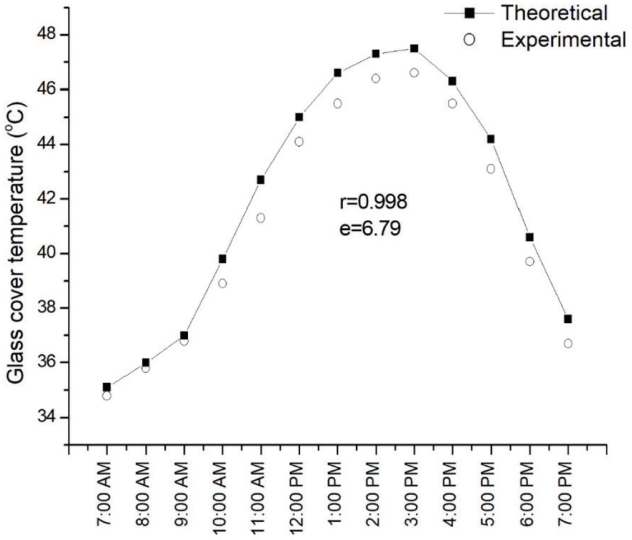

Figure 9. Theoretical and experimental glass temperature.

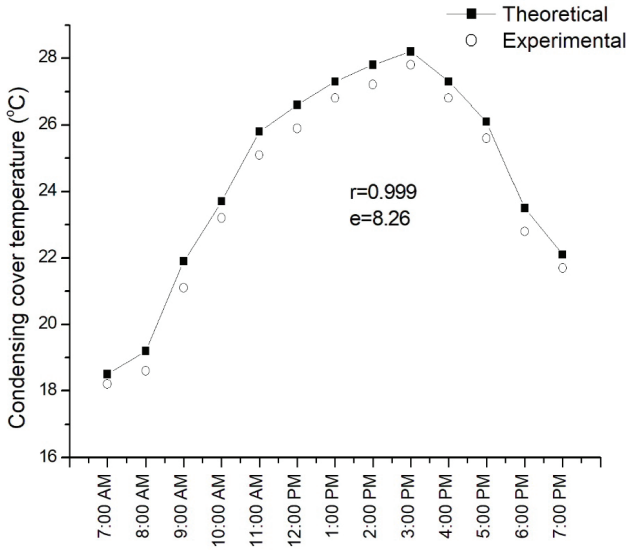

Figure 10. Theoretical and experimental condensing cover temperature.

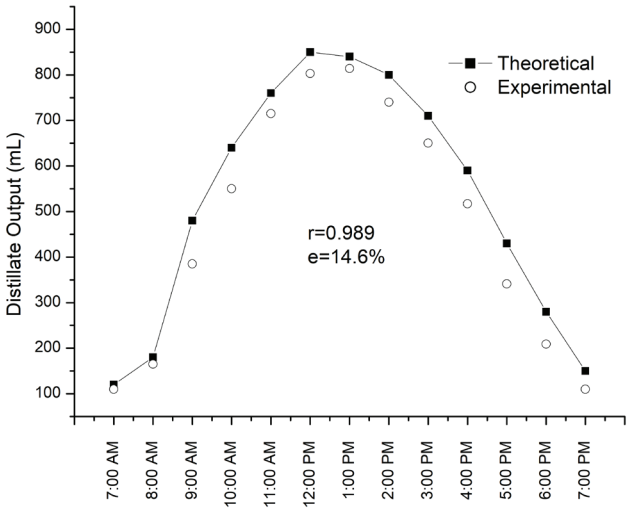

Figure 11. Theoretical and experimental hourly distillate output.

NUMERICAL COMPUTATIONS

Effect of MFR and Depth of Water in Basin

Numerical analysis has been done on the impacts of the water depth in the basin and the mass flow rate (MFR) of water passing over the condensing cover of a solar still (SS). The solar still's total daily distillate output during a summer day was computed. In this analysis, the beginning glass temperature was set at 1°C below the water temperature, and the initial condensing cover temperature was set to the surrounding air's wet bulb temperature (WBT). Furthermore, it was thought that the water's initial temperature was taken same as the surrounding air temperature. These computations were performed for a day (24h) in summer for climate of Raipur, Chhattisgarh, India. Hourly ambient temperature solar radiation and wet bulb temperature for a day in summer is shown in Figure 12.

To analyse the effect of water depth on stills performance MFR is kept constant. The water depth in the basin was varied at 1 cm, 2 cm, 3 cm, 4 cm, 5cm and the MFR of water flowing over the cover was set at 0.065 kg/s. Raipur's average wind speed was considered as 2 m/s (monthly average for May)

As the basin's water depth increased, the daily distillate output slightly decreased (Fig. 13). In particular, the daily

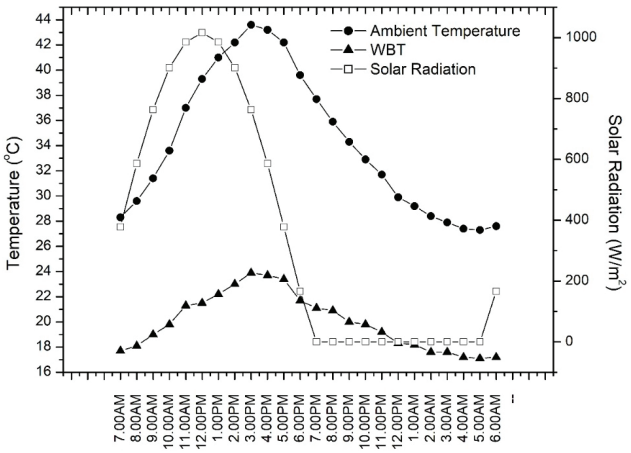

Figure 12. Hourly solar radiation, ambient temperature and WBT of summer (May).

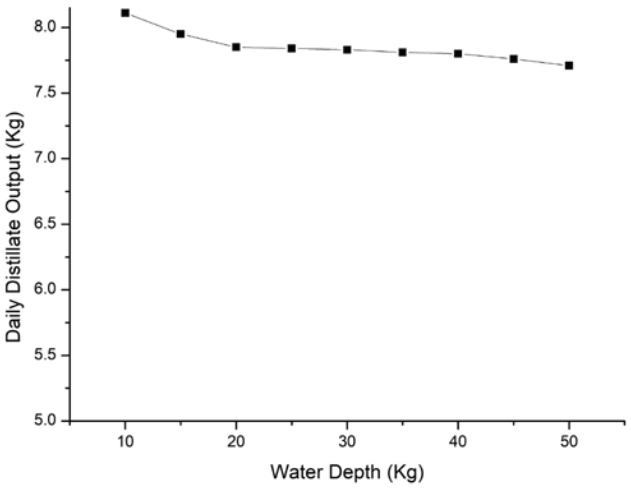

Figure 13. Effect of increasing the depth of water in basin.

distillate output decreased by just 4.9% when the water depth increased from 1 cm to 5 cm. On the other hand, the distillate yield of traditional solar stills (SS) usually decreases more noticeably as the water depth increases. In this design as evaporation and condensation zones are separated and condensation rate is now actively enhanced by flowing cooled water over condenser. The cooled condenser continuously maintains the temperature difference between water and condenser and hence the depth of water does not affect significantly.

Additional numerical calculations were carried out to evaluate the daily distillate output of the proposed design by altering the MFR of water running over the condensing cover in order to examine the impact of the MFR of water flowing over the cover. The basin's water depth was 2 cm, meteorological data considered are same as given above (Fig 14). The effect of changing the MFR of water flowing over the condensing cover was found to be nearly insignificant, as seen in Figure 14. While flowing evaporatively cooled water over cover due to thermal saturation the surface cover temperature of condenser remains low even at lower MFR with increase MFR further does not significantly lower condenser temperature hence distillate output does not increase noticeably.

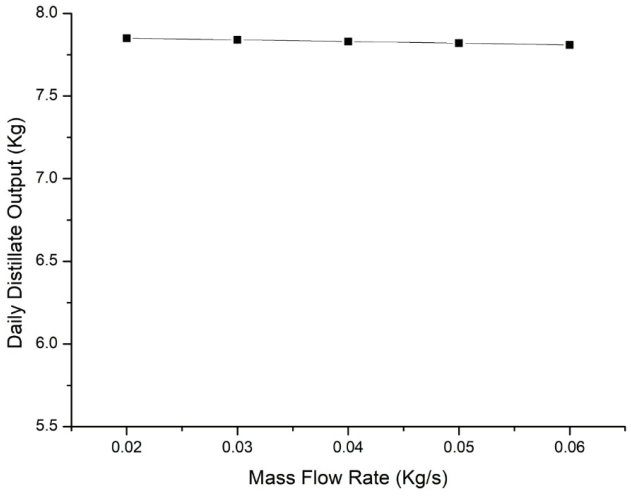

Figure 14. Effect of varying MFR of water flowing over condensing cover.

Effect of Relative Humidity and Wind Velocity

To analyze the effect of relative humidity of ambient air and wind velocity we considered a typical set of parameters to compute hourly yield from the proposed device. For analyzing the effect of relative humidity, we considered ambient temperature as T_a=35°C, I=800W/m² and wind velocity was taken as v_a=2m/s. Numerical computation was performed to determine hourly yield by varying relative humidity from 0.2 to 0.9. The hourly yield with varying relative humidity for typical data set was computed and shown in Figure 15. The result is as expected like other evaporative cooling devices the system works less effectively when the humidity is high. The hourly output decreases with increase in relative humidity of air. The inlet temperature of water flowing through condenser is considered equal to WBT. An increase in ambient humidity raises the wet-bulb temperature of air, thereby reducing the cooling potential and effectiveness of the condenser. For a typical set of parameters when the relative humidity increases from 0.2 to 0.9 the decrease in hourly output is 5.7%.

To study the effect of wind velocity we considered T_a=35°C, I=800W/m² and γ=0.2 Numerical computation was performed to determine hourly yield by varying wind velocity as 1m/s, 2m/s, 3m/s and 4m/s. The hourly yield has been computed at different wind velocity and shown in Figure 16. Unlike conventional solar distillation system were the distillate output increases with increase in wind velocity. Here in this design, we found the slight decrease

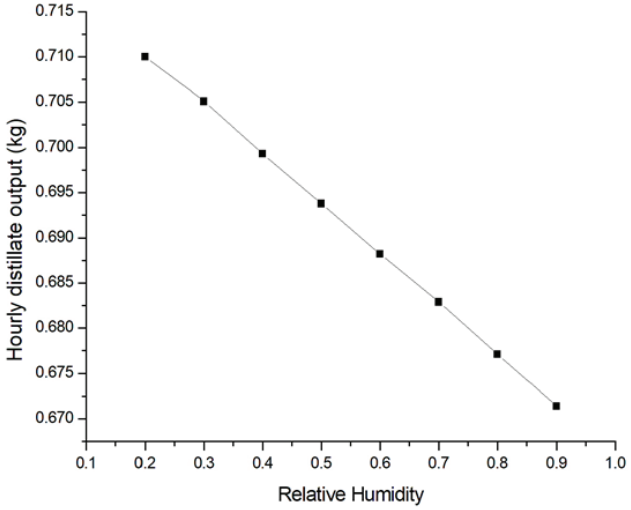

Figure 15. Effect of relative humidity of air on distillate output (T_a=35°C, I=800W/m^2).

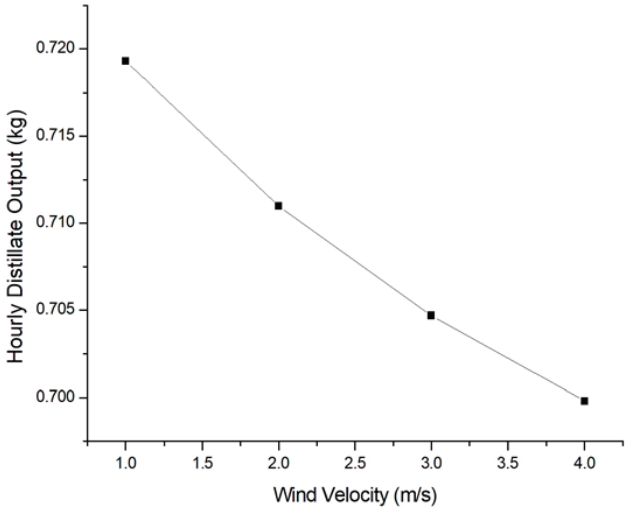

Figure 16. Effect of relative humidity of air on distillate output (T_a=35°C, I=800W/m^2, Relative Humidity=0.2).

in hourly distillate output with the increase in wind velocity. Since the proposed design has a separate condensing unit which is evaporatively cooled by cooled water flowing over it. The condenser is already very effective so the evaporation is more dominating factor. Glass cover gets cooled due to increase in convective coefficient between glass and ambient air. The air inside gets cooled this reduces the greenhouse effect. The rate of evaporation gets reduced at high wind velocity thereby decreases the distillate output produced by system. When the wind velocity increases from 1m/s to 4m/s the decrease in the hourly distillate output is 2.7%.

Performence of the Proposed Design

Numerical computation has been performed to determine the performance of the proposes SS for a summer (May) winter (Jan.) and autumn (Oct.) day in the climate of Raipur Chattisgarh. The climate data for Jan. and Oct. is shown in Figure 17. Slight improvement in output was observed with a lower basin water depth due to enhanced thermal response. Despite this, maintaining an intermediate water depth is recommended to reduce the need for frequent replenishment. Additionally, operating with a reduced MFR of cooling water is advisable, as it minimizes pumping power requirements without significantly compromising productivity. For further computations authors considered depth of water in basin as 2cm and MFR as 0.020kg/s.

The performance of the propose design in May, January and October has been computed. Climate data for (May) is shown in Figure 12. Climate data for January and October

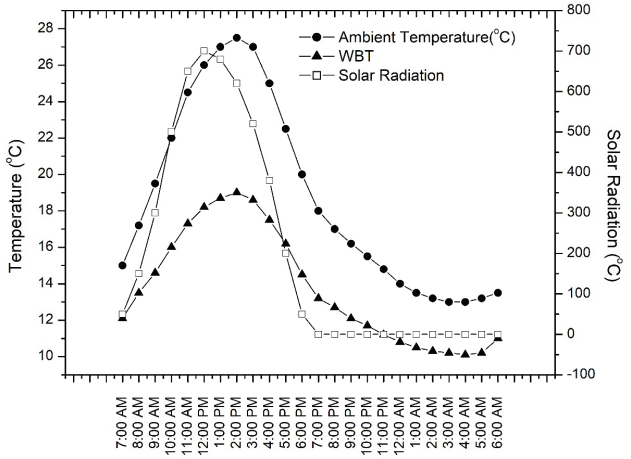

(a)

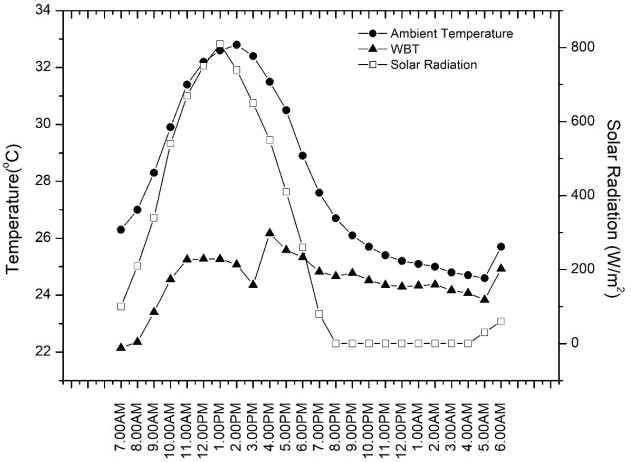

(b)

Figure 17. Climatic data for (a) Winter (Jan.), (b) Autumn (Oct.).

is shown in Figure 16. the total solar radiation received in a day for May, January, and October is 740.3 MJ/m^2, 441.7 MJ/m^2 and 535.7 MJ/m^2. The maximum ambient temperature reached in day for May, January and October is 43.6°C, 27.1°C and 33.4 °C, respectively. Hourly water temperature, temperature of glass cover and condenser cover has been computed and shown in Figure 18,19, and 20.

During the summer month of May, the highest temperature difference between the basin water and the condenser was seen as 29°C around 12:00 PM, resulting in the peak distillate yield of approximately 0.93 kg for that hour. In contrast, during January (winter), the maximum temperature difference reached 26.6°C at 1:00 PM, producing

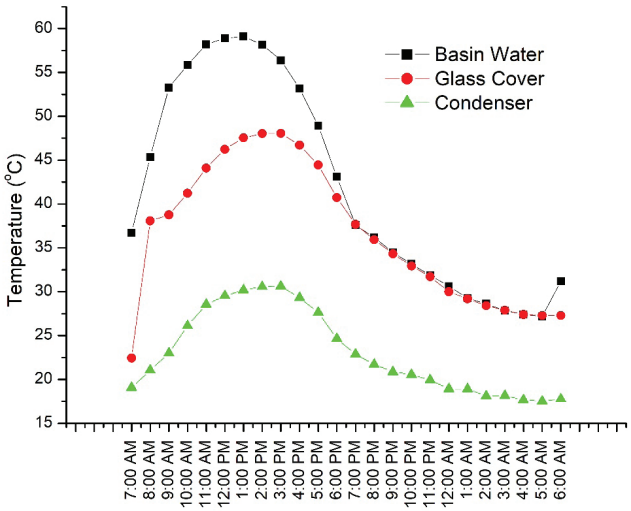

Figure 18. Computed temperature of basin water, glass cover & condenser during summer (May).

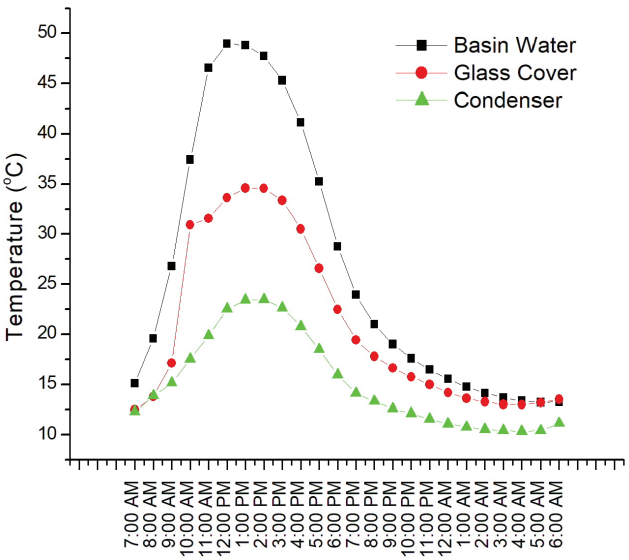

Figure 19. Computed temperature of basin water, glass cover & condenser during winter (January).

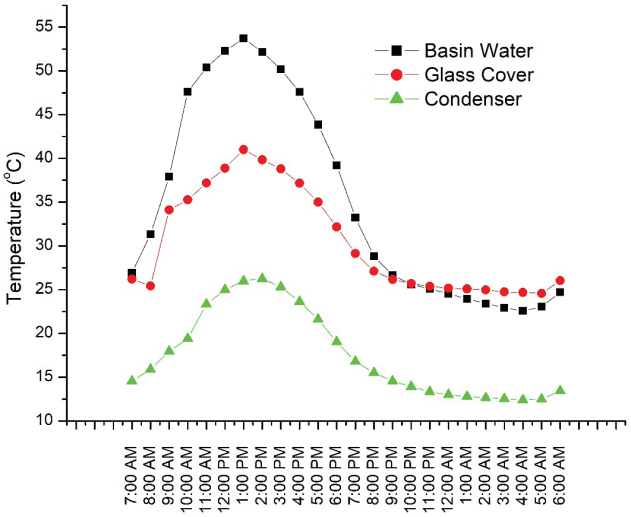

Figure 20. Computed temperature of basin water, glass cover & condenser during autumn (October).

a corresponding maximum hourly distillate output of 0.55 kg. For the month of October, the peak temperature difference of 28.4°C occurred at 2:00 PM, with the associated maximum distillate generation being 0.67 kg per hour.

The continuous cooling of condenser by cooled water helps to maintain the temperature difference between water and condensing cover during day time (6.00AM-6.00PM) as well as in night (6.00PM-6.00AM). This helps to produce distilled water during day as well as during night.

The hourly distillate output produced by the proposed system during different months have been computed and shown in Figures 21, 22 and 23. The total distillate output produced in May, Jan. and Oct.is 7.83kg/day, 3.45kg/day and 5.30kg/day, respectively. The system helps to produce

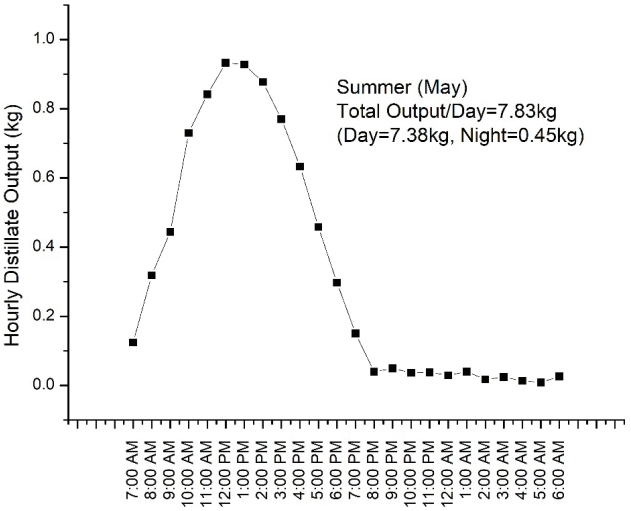

Figure 21. Hourly distillate output produced in a day for May.

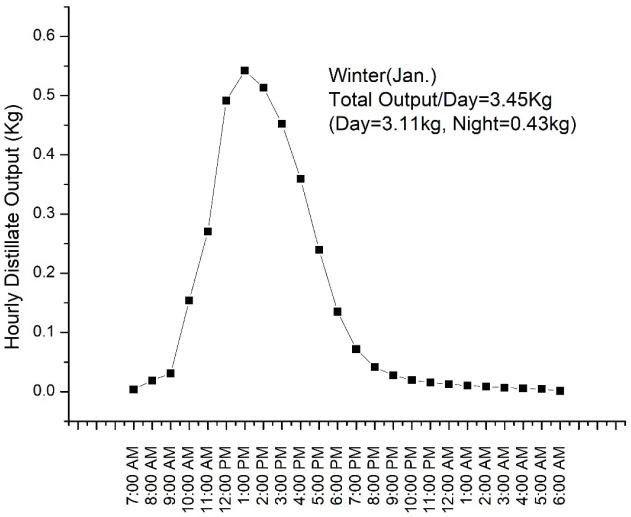

Figure 22. Hourly distillate output produced in a day for January.

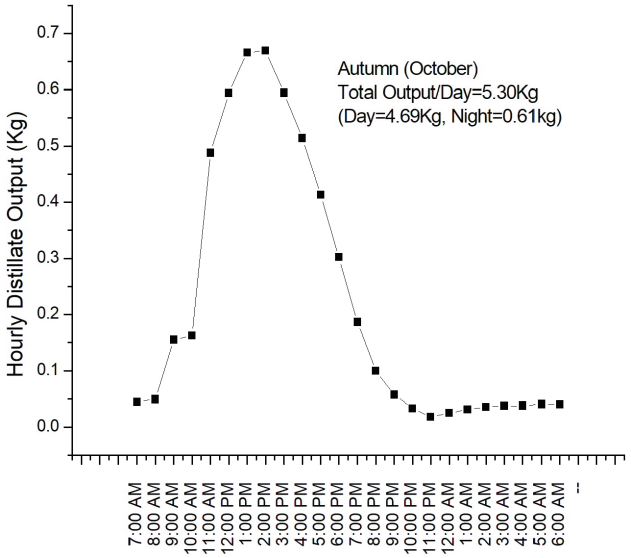

Figure 23. Hourly distillate output produced in a day for October.

some amount of distillate during night time also. The distillate output produced during night for May, Jan. and Oct. are 0.45kg, 0.43kg and 0.61kg, respectively.

Economic Analysis

An economic analysis was conducted to determine the cost per liter of water produced by the proposed solar still (SS). The following assumptions were made for the analysis:

1. The rate of interest (i) is assumed to be 10%, with a total plant life of 20 years.
2. The annual maintenance cost (AMC) is estimated at 12% of the initial annual cost.
3. The salvage value of the plant is considered to be 50% of the total cost of usable items.
4. The cost of items is based on current market prices (as shown in Table-3).
5. The cost of the desert cooler is excluded from the calculation. (Since desert cooler generally used in household for room cooling)
6. The daily water yield is calculated as the average between the yields in summer and winter.
7. The number of clear days in Raipur is taken as 309 days per year
8. The system uses a 5 W PV-powered exhaust fan, and its cost has been accounted for, while its auxiliary energy demand is considered negligible

The *TAC* of the plant will be given by
$TAC = CC \times CRF + AMC - SV \times SFF$
TAC = 2269.9
CRF and *SFF* is given by,

$$CRF = \frac{i(1+i)^n}{(1+i)^n - 1},$$

CRF = 0.117

$$SFF = \frac{i}{(1+i)^n - 1}$$

SFF = 0.017
Cost/L of water produced will be given by,
Cost/Litre = TAC/ TAD = Rs.1.30/L(US$0.015)

Sensitivity Analysis Energy Equivalence and Water Quality

To assess the robustness of the proposed system, a sensitivity analysis was performed considering variations in solar availability and pump reliability. The results (Table 4) show the effect of reduced or enhanced solar radiation (±25%) and pump failure scenarios (10% and 20% downtime) on annual water output, cost of water, and payback period. We considered sensitivity scenario based on seasonal bands:

Table 3. Details of items

S. No	Material	Cost
1	M.S. Sheet (1.5mm)	Rs. 6265.35 (72.62 US$)
2	Glass (4 mm) 1m^2	Rs. 320 (3.71 US$)
3	Condenser plate (Aluminum 1m^2)	Rs. 220 (2.55 US$)
4	Solar fan (5W)	Rs. 250 (2.90 US$)
5	Solar pump	Rs. 550 (6.37 US$)
6	Putty	Rs. 60 (0.70 US$)
7	Pipes fittings (valve, etc.)	Rs. 400 (4.64 US$)
8	Mics.	Rs. 500 (5.79 US$)
	Total	**Rs. 8565.35 (99.27 US$)**

(i) Winter (low) representative winter solar availability and ambient conditions (ii) Annual-average (base); and (iii) Summer(high) representative summer conditions. Outputs are computed with the same model using seasonal inputs. While higher insolation generally increases yield, productivity does not scale strictly linearly due to seasonal changes in (Tw–Tc) and convective losses. The payback period (PBP) will be given by

PBP=CC/Annual Net Saving

Annual Net Saving = (Annual Distillate Output) x (Selling Price)

In pump failure scenario the system still run as conventional solar distillation system having separate condenser without cooling. The daily distillate output considered with pump failure as 3kg/day

The analysis indicates that although the total annual cost remains constant, lower output under adverse conditions increases the unit cost of water and extends the payback period, whereas favourable conditions shorten it. For different scenario discussed in table the cost/kg of water produced is between Rs 0.94/kg to Rs 1.43/kg and the payback period between 0.236-0.535year.

`In addition, an energy equivalence analysis was carried out (Table 5) to quantify the environmental benefit of the system under the same scenarios. The annual distillate output was converted into equivalent energy savings, coal displaced, and associated CO_2 emissions avoided. This parallel evaluation highlights both the economic feasibility and sustainability advantage of the system, demonstrating its potential for potable water generation even under variable operating conditions. Energy equivalence (Q_E) and the mass of coal burned (M_c) will be given by,

$$Q_E(kWh) = \frac{(Anualloutput)L}{3600}$$

$$M_c = \frac{Q_E \times 3600}{(CV)_{coal} \times \eta_{plant}}$$

In above Equation $(CV)_{coal}$ calorific value of coal is taken as 20,000KJ/kg and plant efficiency η_{plant} is considered 0.35. The energy equivalence analysis shows that the system can significantly offset coal consumption and associated CO_2 emissions. Depending on the operating scenario, the

Table 4. Sensitivity Analysis (Selling Price /kg=Rs15)

Case	Solar availability	Pump availability	Annual water output	Cost/kg	Payback (year)
Base (Average)	100%	100%	1742.8 kg	Rs1.30/kg	0.327
Higher (Summer)	125%	100%	2419.5 kg	Rs0.94/kg	0.236
Lower (Winter)	75%	100%	1066.0 kg	Rs2.12/kg	0.535
Pump Failure (30 days/Year)	100%	90%	1663.6 kg	Rs1.36/kg	0.343
Pump Failure (60 days/Year)	100%	80%	1584.4 kg	Rs1.43/kg	0.360

Table 5. Energy equivalence of distillate output

Case	Annual distillate output	Energy equivalence	Equivalent coal burned (kg)	Co_2 emission avoided (kg) 0.65 kg Co_2/(kWh)
Base	1742.8 kg	1094 kWh	563 kg	711 kg
Higher	2419.5 kg	1519 kWh	781 kg	987 kg
Lower	1066.0 kg	669 kWh	344 kg	435 kg
Pump failure (30days)	1663.6 kg	1045 kWh	538 kg	350 kg
Pump failure (60days)	1584.4 kg	995 kWh	512 kg	647 kg

Table 6. Chemical analysis of distillate water compared with WHO standards

Parameters	Distillate	WHO limits	Remarks
pH	7.1	6.5-8.5	Safe
TDS (mg/L)	12	<500	Very Low
Hardness (mg/L as $CaCO_3$)	6	<200	Very Soft
Bacteria	Nil	0	Safe

annual freshwater yield corresponds to an energy saving of about 669–1519 kWh, which is equivalent to avoiding the burning of 344–781 kg of coal and reducing 435–987 kg of CO_2 emissions

To check the quality of water produced by the system a chemical analysis has been performed and shown in Table 6. It is seen that the water produced is fit for drinking fulfilling all recommendations limits as prescribed by WHO.

CONCLUSION

The proposed design of SS contains two different sections separated by a common plate the section towards left is called evaporative section and two the right is called as condenser section. The water vapours produced in the evaporator section is forced towards condensing section by a low power exhaust fan in between. The condenser plate is evaporatively cooled by flowing cooled tank water from an air cooler. The cooled condenser behaves as a heat sink

Table 7. Summary of solar still modifications integrated with passive condensers

Reference	Modification	Operating Condition	Key Result	Unique Feature / Novelty
Fath et al. [23]	Single-slope still with passive condenser; studied diffusion, purging, and circulation.	Hot/arid climate; ~800 W/m²	70% increase in yield	Passive condenser integration
Fath et al. [33]	Natural convection-based humidification system with built-in condenser.	Laboratory; ~700–800 W/m²	5.1 kg/m²·day output	Humidification–dehumidification system
Madhlopa & Johnstone [34]	External condenser with added basin areas.	Malawi; ~850 W/m²	Up to 60% gain	Multi-basin + external condenser
Monowe et al. [35]	Portable still with external condenser and reflector.	Field test; ~850–900 W/m²	5–8 L/m²·day output	Portable + reflector-assisted
Kabeel et al. [45]	Used external condenser with Al_2O_3 nanofluid.	Egypt; ~850 W/m²	Up to 116% enhancement	Nanofluid-based heat transfer
Al-Nimr & Al-Ammari [46]	PV/T-integrated still with external finned condenser.	700 W/m² solar input	7.9 kg/m²·day	PV/T integration with finned condenser
Rabhi et al. [47]	Still with pin-finned absorber and condenser.	Tunisia; ~850 W/m²	43.7% efficiency	Pin-finned absorber plate
Belhadi et al. [48]	Double-slope still with capillary film condenser.	Mediterranean climate	7.15 kg/m²·day	Capillary film condenser
Kumar et al. [49]	Single-slope still with external condenser.	Semi-arid climate	39.4% higher yield	Conventional SS + external condenser
Bhardwaj et al. [38]	Inflatable still with household-type passive condenser.	Lab conditions	~0.75 L/h output	Inflatable structure
Hassanaa & Abo-Elfadl [50]	Tested various condensers and saline water types.	Lab & seasonal tests	Max 52% gain with heat sink + steel fibers	Different condenser materials tested
Rahmani & Boutriaa [39]	NCL-driven condenser under seasonal changes.	Algeria; summer & winter	4.73 (summer), 2.71 (winter) kg/m²·day	Natural circulation loop condenser
Saini et al. [51]	PV-powered still with passive condenser and fan.	India; ~800 W/m²	Enhanced yield and efficiency	PV-driven fan for improved cooling
Rashid et al. [6]	Review of floating solar stills and floating solar-driven membranes.	Global review	Yields often exceed land-based SS; modular & scalable	Floating platforms reduce heat loss, allow hybridization
Hussein et al. [7]	Comprehensive review of inverted solar still designs and models.	Global review	Yields up to 11 kg/m²·day in modified inverted systems	Inverted geometry improves absorptivity & reduces losses
Al-Obaidi et al. [8]	Review of hybrid membrane + thermal desalination powered by fossil fuels.	Global review	Higher recovery & efficiency, but high energy/GHG cost	Future focus: renewables + hybridization
Present Work	Solar still with evaporatively cooled condenser (SS + air cooler).	India; May (Summer), ~850–900 W/m²	7.83 kg/day; cost US $0.015/kg	Evaporatively cooled condenser with low-cost operation

and thus helps to condense more quantity of vapours this enhances the overall distillate output of the system. The present work proposes the overall thermal performance analysis of this system. During the study the conclusions drawn are as follows: -

1. The mathematical model of the design has been developed and validated by experiment in Raipur, Chhattisgarh, India (21°14′40″N and 81°37′50″E)
2. As the basin water depth increased, a slight reduction in daily distillate output was observed. Specifically, when the water depth increased from 1 cm to 5 cm, the daily distillate yield decreased by only 4.9%
3. The mass flow rate of water flowing over the condenser plate has negligible affect on the distillate output produced.
4. For a typical set of parameters, it is seen that the hourly distillate output decreases by 5.7% when the relative humidity of air increased from 0.2 to 0.9
5. With increases in wind velocity from 1m/s to 4m/s the hourly distillate output decreases by 2.7 %.
6. Considering 2cm depth of water in basin and at mass flow rate of 0.020kg/s the system generates 7.83kg/day, 3.44kg/day and 5.30 kg/day total distillate for a day in May, Jan. and Oct. The total radiation received for a day in May, Jan and Oct. is 740.3MJ/m^2, 441.7MJ/m^2 and 535.7MJ/m^2, respectively.
7. The system is capable of generating distilled water even during nighttime due to the effective cooling provided by the separate condenser. The distillate output produced during night (6.00PM-6.00AM) is 0.45kg/m^2, 0.43kg/m^2 and 0.61kg/m^2 for a day in months of May, Jan. and Oct. This output represents an additional benefit, as it utilizes the stored heat without requiring significant extra energy input apart from minimal auxiliary power. While this quantity is modest, it can still contribute to daily freshwater availability, particularly in water-scarce areas
8. The cost of water produced is Rs 1.30/L (US$ 0.015/L)

Applicability of the Proposed Design

- Rural Households: The system's low maintenance, passive solar powered, and simple construction make it suitable for decentralized water purification in rural areas lacking reliable potable water access.
- Off-grid Communities: Since the system operates without electrical power (except minimal pumping for condenser cooling, which can be solar-powered), it is highly suitable for off-grid or remote communities where grid access is limited.
- Disaster Relief: The compact design, ability to produce clean water using only solar energy and minimal infrastructure, makes it a promising option for rapid deployment during natural disasters or emergency relief operations.

Additionally, we have estimated daily water output under typical rural solar insolation conditions, indicating that the unit can provide 3–8 liters/day, which is sufficient for basic drinking water needs of a small family. A comparison table (Table-7) has been given to compare the present work with some past works on solar distillation system having separate condenser. When compared we found that the proposed system works reasonably well to fulfill the pure water requirements of small communities in rural areas.

Limitation of the present work

1. Economic analysis did not include the cost of the air cooler, as it was assumed to be a pre-existing household appliance. In communities without coolers, the overall cost and payback period would be higher.
2. Scale formation effects were not studied. In hard-water areas, scaling can reduce heat transfer efficiency. Practical adoption will require mitigation strategies such as cleaning, water softening, or anti-sealant coatings.
3. Implementation aspects such as user training, large-scale deployment, and socio-economic challenges were beyond the scope of this work. These will be addressed through field trials and user studies in future work.

NOMENCLATURES

A_b	Area of basin, m^2
A_g	Area of glass cover, m^2
A_c	Area of condensing plate, m^2
c_w	Specific heat of water, $Jkg^{-1}K^{-1}$
h_i	Total internal heat transfer coefficient, W / m^2K
h_0	Total external heat transfer coefficient, W / m^2K
h_2	Sum of convective & radiative heat transfer coefficient between water and water film, W / m^2K
h_{rw}	Radiative heat transfer coefficient between water and glass cover, W / m^2K
h_{cw}	Convective heat transfer coefficient between water and glass cover, W / m^2K
h_{ew}	Evaporative heat transfer coefficient between water and glass cover, W / m^2K
h_{ca}	Convective heat transfer coefficient between glass and air, W / m^2K
h_{ra}	Radiative heat transfer coefficient between glass and air, W / m^2K
h_b	Heat transfer coefficient between basin liner and water, W / m^2K
h_f	Convective heat transfer coefficient between condensing plate and water film, W / m^2
i	Annual rate of interest
Lv	Latent heat of vapourization of water, J / kg
$\dot{m}_f$	Mass flow rate of water flowing over condensing plate (film flow rate), kg / s
$\dot{m}_{ew}$	Distillate output produced per hour, kg / h
M_w	Mass of water in basin of solar still, kg
P_w	Saturated vapour pressure at water temperature, N / m^2
P_g	Saturated vapour pressure at glass temperature, N / m^2
$\dot{Q}_u$	Rate of heat added by solar still into tank, W

$\dot{Q}_m$ Rate of heat taken by make-up water, W
$\dot{Q}_T$ Rate of heat loss from top of storage tank, W
$\dot{Q}_s$ Rate of heat loss from sides of storage tank, W
$\dot{Q}_b$ Rate of heat loss from bottom of storage tank, W
q_{rw} Rate of radiative heat transfer from water to glass, W
q_{cw} Rate of convective heat transfer from water to glass, W
q_{ew} Rate of evaporative heat transfer from water to glass, W
q_{ca} Rate of convective heat transfer from glass to air, W
q_{ra} Rate of radiative heat transfer from glass to air, W
$\dot{q}_{cf}$ Rate of convective heat transfer from condensing plate to film, W
$\dot{q}_{cfa}$ Rate of convective heat transfer from film to air, W
$\dot{q}_{rfa}$ Rate of radiative heat transfer from film to air, W
I Solar radiation, W / m^2
T_g Temperature of glass cover, °C
T_w Temperature of water in basin, °C
T_a Ambient temperature, °C
T_b Temperature of basin liner, °C
T_{w0} Initial water temperature, °C
T_{wt} Tank (reservoir) water temperature, °C
T_{wl_n} Exit water temperature from nth row of plant, °C
U_s Side loss coefficient of the storage tank, $Wm^{-2}K^{-1}$
U_t Top loss coefficient of the storage tank, $Wm^{-2}K^{-1}$
U_b Bottom loss coefficient of the storage tank, $Wm^{-2}K^{-1}$
v_a Velocity of air, m/s
α_g Absorptivity of glass cover
σ Stefans-Boltzmann constant, W / m^2K^4
ρ_w Density of water, kg / m^3

Abbreviations

SS Solar still
MFR Mass flow rate
TAC Total annual cost
TAD Total annual distillate produced
CC Capital cost
CRF Capital recovery factor
AMC Annual maintenance cost
SV Salvage value
SFF Sinking fund factor
CF Cash flow
U Uncertainty
WBT Wet bulb temperature

REFERENCES

[1] Awasthi A, Kumari K, Panchal H, Sathyamurthy R. Passive solar still: Recent advancements in design and related performance. Environ Technol Rev 2018;7(1):235-261. [CrossRef]

[2] Durkaieswaran P, Murugavel KK. Various special designs of single basin passive solar still - A review. Renew Sustain Energy Rev 2015;49:1048-1060. [CrossRef]

[3] Murugavel KK, Chockalingam KKSK, Srithar K. Progresses in improving the effectiveness of the single basin passive solar still. Desalination 2008;220(1-3):677-686. [CrossRef]

[4] Ansari O, Asbik M, Bah A, Arbaoui A, Khmou A. Desalination of the brackish water using a passive solar still with a heat energy storage system. Desalination 2013;324:10-20. [CrossRef]

[5] Sarkar Md NI, Sifat AS, Reza SMS, et al. A review of optimum parameter values of a passive solar still and a design for southern Bangladesh. Renew Wind Water Solar 2017;1:1-13. [CrossRef]

[6] Rashid FL, Al-Obaidi MA, Hussein AK, Akkurt N, Ali B, Younis O. Floating solar stills and floating solar-driven membranes: Recent advances and overview of designs, performance and modern combinations. Sol Energy 2022;247:355-372. [CrossRef]

[7] Hussein AK, Rashid FL, Abed AM, Al-Khaleel M, Togun H, Ali B, et al. Inverted solar stills: A comprehensive review of designs, mathematical models, performance, and modern combinations. Sustainability 2022;14:13766. [CrossRef]

[8] Al-Obaidi MA, Alsarayreh AA, Rashid FL, Sowgath MT. Hybrid membrane and thermal seawater desalination processes powered by fossil fuels: A comprehensive review, future challenges and prospects. Desalination 2024;583:117694. [CrossRef]

[9] Al-Obaidi MA, Alsarayreh AA, Rashid FL, Sowgath MT, Alsadaie S, Ruiz-García A, et al. Hybrid membrane and thermal seawater desalination processes powered by fossil fuels: A comprehensive review, future challenges and prospects. Desalination 2024;583:117694. [CrossRef]

[10] Rashid FL, Shareef AS, Alwan HF. Enhancement of fresh water production in solar still using new phase change materials. J Adv Res Fluid Mech Therm Sci 2019;61:63-72.

[11] Chaichan MT, Kazem HA. Water solar distiller productivity enhancement using concentrating solar water heater and phase change material (PCM). Case Stud Therm Eng 2015;2:24-31. [CrossRef]

[12] Rashid FL, Al-Obaidi MA, Hussein AK, Akkurt N, Ali B, Younis O. Floating solar stills and floating solar-driven membranes: Recent advances and overview of designs, performance and modern combinations. Sol Energy 2022;247:355-372. [CrossRef]

[13] Hussein AK, Rashid FL, Rasul MK, Basem A, Younis O, Homod RZ, et al. A review of the application of hybrid nanofluids in solar still energy systems and guidelines for future prospects. Sol Energy 2024;272:112485. [CrossRef]

[14] Rashid FL, Al-Obaidi MA, Mohammed HI, Togun H, Ahmad S, Ameen A. A review of the current situation and prospects for nanofluids to improve solar still performance. J Therm Anal Calorim 2024;149(23):13511-13531. [CrossRef]

[15] Hidouri K, Togun H, Rashid FL, Abed AM, Hussein AK, Ali B, et al. Environmental studies for various simple and hybrid solar still configurations: A comprehensive review. J Therm Eng 2024;10(6):1698-1714. [CrossRef]

[16] Ajit A, Pandey H, Gupta NK. Analysis of solar water desalination using hybrid nanofluids: An experimental study. J Therm Eng 2023;9(6):1502-1515. [CrossRef]
[17] Chauhan MK, Chauhan AK, Khan Y, Singh AP. Experimental and theoretical investigation of thermal efficiency and productivity of single slope basin type solar distillation system using honey-comb. J Therm Eng 2021;9(6):1559-1571. [CrossRef]
[18] Tiwari GN. Solar Energy: Fundamentals, Design, Modelling and Applications. Alpha Science Int'l Ltd; 2002.
[19] Gaur MK, Norton B, Tiwari GN, editors. Solar Thermal Systems: Thermal Analysis and Its Application. Bentham Science Publishers; 2022. [CrossRef]
[20] Tiwari A, Tiwari GN. Solar Distillation Practice for Water Desalination Systems. Anshan; 2008.
[21] Tiwari GN, Sahota L. Advanced Solar-Distillation Systems: Basic Principles, Thermal Modeling, and Its Application. Autumner; 2017. [CrossRef]
[22] Tiwari GN, Tiwari A. Handbook of Solar Energy. Vol. 498. Singapore: Autumner; 2016. [CrossRef]
[23] Fath HES, Elsherbiny SM. Effect of adding a passive condenser on solar still performance. Energy Convers Manag 1993;34:63-72. [CrossRef]
[24] Fath HES, Hosny HM. Thermal performance of a single-sloped basin still with an inherent built-in additional condenser. Desalination 2002;142:19-27. [CrossRef]
[25] ElSherbini A, Maheshwari GP. Effectiveness of shading air-cooled condensers of air-conditioning systems. 2010. [CrossRef]
[26] Mugisidi D, Fajar B, Syaiful S, Utomo T. Solar still with an integrated conical condenser. CFD Lett 2023;15(8):122-134. [CrossRef]
[27] Bhardwaj R, ten Kortenaar MV, Mudde RF. Maximized production of water by increasing area of condensation surface for solar distillation. Appl Energy 2015;154:480-490. [CrossRef]
[28] Mohaisen HS, Esfahani JA, Ayani MB. Improvement in the performance and cost of passive solar stills using a finned-wall/built-in condenser: An experimental study. Renew Energy 2021;168:170-180. [CrossRef]
[29] Mevada D, Panchal H, Nayyar A, Sharma K, Manokar AM, El-Sebaey MS, et al. Experimental performance evaluation of solar still with zig-zag shape air cooled condenser: An energy-exergy analysis approach. Energy Rep 2023;10:1198-1210. [CrossRef]
[30] E1-Bahi A, Inan D. A solar still with minimum inclination, coupled to an outside condenser. Desalination 1999;123:79-83. [CrossRef]
[31] Toosi SSA, Goshayeshi HR, Heris SZ. Experimental investigation of stepped solar still with phase change material and external condenser. J Energy Storage 2021;40:102681. [CrossRef]
[32] Tuly SS, Rahman MS, Sarker MRI, Beg RA. Combined influence of fin, phase change material, wick, and external condenser on the thermal performance of a double slope solar still. J Clean Prod 2021;287:125458. [CrossRef]
[33] Fath HES, Elsherbiny S, Ghazy A. A naturally circulated humidifying/dehumidifying solar still with a built-in passive condenser. Desalination 2004;169(2):129-149. [CrossRef]
[34] Madhlopa A, Johnstone C. Numerical study of a passive solar still with separate condenser. Renew Energy 2009;34(7):1668-1677. [CrossRef]
[35] Monowe P, Masale M, Nijegorodov N, Vasilenko V. A portable single-basin solar still with an external reflecting booster and an outside condenser. Desalination 2011;280(1-3):332-338. [CrossRef]
[36] Kabeel AE, Omara ZM, Essa FA. Numerical investigation of modified solar still using nanofluids and external condenser. J Taiwan Inst Chem Eng 2017;75:77-86. [CrossRef]
[37] Rabhi K, Nciri R, Nasri F, Ali C, Bacha HB. Experimental performance analysis of a modified single-basin (SSSS) with pin fins absorber and condenser. Desalination 2017;416:86-93. [CrossRef]
[38] Bhardwaj R, ten Kortenaar MV, Mudde RF. Inflatable plastic solar still with passive condenser for single family use. Desalination 2016;398:151-156. [CrossRef]
[39] Rahmani A, Boutriaa A. Numerical and experimental study of a passive solar still integrated with an external condenser. Int J Hydrog Energy 2017;42(48):29047-29055. [CrossRef]
[40] Kabeel AE, Harby K, Abdelgaied M, Eisa A. A comprehensive review of tubular solar still designs, performance, and economic analysis. J Clean Prod 2020;246:119030. [CrossRef]
[41] Saini V, Sahota L, Jain VK, Tiwari GN. Performance and cost analysis of a modified built-in-passive condenser and semitransparent photovoltaic module integrated passive solar distillation system. J Energy Storage 2019;24:100809. [CrossRef]
[42] Somwanshi A, Tiwari AK. Performance enhancement of a single basin solar still with flow of water from an air cooler on the cover. Desalination 2014;352:92-102. [CrossRef]
[43] Tiwari AK, Somwanshi A. Techno-economic analysis of mini solar distillation plants integrated with reservoir of garden fountain for hot and dry climate of Jodhpur (India). Sol Energy 2018;160:216-224. [CrossRef]
[44] Sodha MS, Somwanshi A. Variation of water temperature along the direction of flow: Effect on performance of an evaporative cooler. J Fundam Renewable Energy Appl 2012;2:1-6. [CrossRef]
[45] Kabeel AE, Omara ZM, Essa FA. Enhancement of modified solar still integrated with external condenser using nanofluids: An experimental approach. Energy Convers Manag 2014;78:493-498. [CrossRef]

[46] Al-Nimr MA, Al-Ammari W. A novel hybrid PV-distillation system. Sol Energy 2016;135:874-883. [CrossRef]
[47] Rabhi K, Nciri R, Nasri F, Ali C, Bacha HB. Experimental performance analysis of a modified single-basin single-slope solar still with pin fins absorber and condenser. Desalination 2017;416:86-93. [CrossRef]
[48] Belhadj MM, Bouguettaia H, Marif Y, Zerrouki M. Numerical study of a double slope solar still coupled with capillary film condenser in south Algeria. Energy Convers Manag 2015;94:245-252. [CrossRef]
[49] Kumar RA, Esakkimuthu G, Murugavel KK. Performance enhancement of a single basin single slope solar still using agitation effect and external condenser. Desalination 2016;399:198-202. [CrossRef]
[50] Hassan H, Abo-Elfadb S. Effect of the condenser type and the medium of the saline water on the performance of the solar still in hot climate conditions. Desalination 2017;417:60-68. [CrossRef]
[51] Saini V, Sahota L, Jain VK, Tiwari GN. Performance and cost analysis of a modified built-in-passive condenser and semitransparent photovoltaic module integrated passive solar distillation system. J Energy Storage 2019;24:100809. [CrossRef]

APPENDIX I

$$K_1=\frac{H_1U_b+H_2h_o+h_{ew}}{M_wc_w} \qquad K_2=\frac{\tau_1H_2I+\tau_2I+\tau_3H_1I+H_1U_bT_a+H_2h_oT_a}{M_wc_w} \qquad K_3=\frac{h_{ew}}{M_wc_w}$$

$$K_4=\frac{K_2}{K_1}(1-e^{-K_1t})+T_{w0}e^{-K_1t} \qquad K_5=\frac{K_3}{K_1}(1-e^{-K_1t}) \qquad K_6=\frac{h_{ew}K_4}{h_f+h_{ew}-h_{ew}K_5} \qquad K_7=\frac{h_f}{h_f+h_{ew}-h_{ew}K_5}$$

$$A=\frac{0.013h_{cfa}.R_1b}{\dot{m}_fc_w} \qquad B=\frac{b}{\dot{m}_fc_w}(h_fK_7-h_f-h_2-0.013h_{cfa}R_2) \qquad H_1=\frac{h_b}{h_b+U_b}$$

$$H_2=\frac{h_i}{h_i+h_o} \qquad C=\frac{b}{\dot{m}_fc_w}(h_fK_6+h_2T_a-0.013h_{cfa}R_3+0.013h_{cfa}\gamma R_1T_a^{\,2}+0.013h_{cfa}\gamma R_2T_a+0.013\gamma h_{cfa}R_3)$$

APPENDIX II [18]

$$h_{ra}=\varepsilon_g\sigma\left[\frac{(T_g+273)^4-(T_a+261)^4}{T_g-T_a}\right] \qquad h_{ca}=2.8+3v_a \qquad P_w=\exp\left[25.317-\left(\frac{5144}{273+T_w}\right)\right]$$

$$h_{rw}=\varepsilon_{eff}\sigma[(T_w+273)^2+(T_g+273)^2](T_w+T_g+546) \qquad P_g=\exp\left[25.317-\left(\frac{5144}{273+T_g}\right)\right]$$

$$h_{cw}=0.884[(T_w-T_{g/c})+\frac{(P_w-P_{g/c})(T_w+273)}{(268.9\times10^3-P_w)}]^{1/3} \qquad \frac{1}{\varepsilon_{eff}}=\frac{1}{\varepsilon_w}+\frac{1}{\varepsilon_g}-1$$

$$h_{ew}=16.273\times10^3h_{cw}\frac{(P_w-P_c)}{(T_w-T_c)} \qquad h_b=135 \qquad h_f=135$$